

# Opinion dynamics in two dimensions: domain coarsening leads to stable bi-polarization and anomalous scaling exponents

F. Velásquez-Rojas and F. Vazquez

IFLYSIB, Instituto de Física de Líquidos y Sistemas Biológicos (UNLP-CONICET),  
1900 La Plata, Argentina

E-mail: fede.vazmin@gmail.com

**Abstract.** We study an opinion dynamics model that explores the competition between persuasion and compromise in a population of agents with nearest-neighbor interactions on a two-dimensional square lattice. Each agent can hold either a positive or a negative opinion orientation, and can have two levels of intensity –moderate and extremist. When two interacting agents have the same orientation become extremists with persuasion probability  $p$ , while if they have opposite orientations become moderate with compromise probability  $q$ . These updating rules lead to the formation of same-opinion domains with a coarsening dynamics that depends on the ratio  $r = p/q$ . The population initially evolves to a centralized state for small  $r$ , where domains are composed by moderate agents and coarsening is without surface tension, and to a bi-polarized state for large  $r$ , where domains are formed by extremist agents and coarsening is driven by curvature. Consensus in an extreme opinion is finally reached in a time that scales with the population size  $N$  and  $r$  as  $\tau \simeq r^{-1} \ln N$  for small  $r$  and as  $\tau \sim r^2 N^{1.64}$  for large  $r$ . Bi-polarization could be quite stable when the system falls into a striped state where agents organize into single-opinion horizontal, vertical or diagonal bands. An analysis of the stripes dynamics towards consensus allows to obtain an approximate expression for  $\tau$  which shows that the exponent 1.64 is a result of the diffusion of the stripe interfaces combined with their roughness properties.

## 1. Introduction

In 1964, Abelson [1] used a mathematical model to pose a puzzle that still intrigues theoretical social scientists. He demonstrated that convergence on “monoculture”, an overall opinion consensus at the population level, is inevitable in a connected population of individuals that continuously update their views by moving towards the average opinion of their neighbors. However, extensive research on opinion formation shows that most empirical opinion patterns resembles those of bi-polarization, rather than those of consensus [1]. The phenomenon of bi-polarization is defined as the development of two groups with antagonistic opinions that intensify their differences over time, and where positions between the two extremes of the opinion spectrum are increasingly less occupied (see [2] for a recent review). The theoretical inevitability of consensus, poorly supported by empirical observations, lead Abelson to wonder: “What on earth one must assume in order to generate the bimodal outcome of community cleavage studies?”. This is one of the long standing questions in theoretical sociology. In the same line, Bonacich and Lu [3] have recently noted that many models show how groups arrive to consensus, but there are not generally accepted models of how groups become polarized or how two groups can become more and more different and possible hostile. Some models that combine positive and negative social influence [4, 5, 6] lead to a bimodal opinion distribution that could explain bi-polarization. However, negative influence is not fully supported by empirical evidence.

Based on previous works [7], Mäs and Flache have recently proposed in Refs. [2, 8] an alternative mechanism that combines homophily [9, 10] with “persuasion argument theory” (PAT) [11, 12, 13], which gives rise to bi-polarization without the assumption of negative influence. The authors have also performed group-discussion experiments to test the validity of the theoretical model. The idea is that, due to homophily an individual tends to interact and talk with a partner that holds the same opinion orientation on a given issue, as for instance to be in favor of the same-sex marriage. Then, PAT suggests that the two interacting individuals are likely to exchange different arguments that support their positions, and thus they can provide each other with new arguments or reasons which reinforce their initial opinions. This could intensify the individuals’ views and make them more extreme in their believes. Motivated by this work, La Rocca et al. [14] have recently introduced a model that incorporates the mechanisms of homophily and persuasion in a simple way, and that is able to generate desired levels of bi-polarization. We refer to this model as the “M-model” from now on. The opinion of each agent is represented by an integer number  $k$  bounded in the interval  $[-M, M]$  ( $k \neq 0$ ) that describes its degree of agreement on a political issue, from totally against ( $k = -M$ ) to totally in favor ( $k = M$ ). Each agent is allowed to interact with any other agent in the population, which corresponds to a mean-field (MF) setup (all-to-all interactions). Two interacting agents with the same orientation (positive or negative) reinforce their opinions in one unit and become more extremists with persuasion probability  $p$ , while the opinions of two interacting agents with opposite

orientations get two units closer with compromise probability  $q$ . It was shown in [14] that the behavior of the model depends on the relative frequency between same-orientation (persuasion) and opposite-orientation (compromise) interactions, determined by the ratio  $p/q$ . When persuasive events are more frequent than compromise events, opinions are driven towards extreme values  $k = -M$  and  $k = M$ , inducing the coexistence of extreme opinions or bi-polarization. In the opposite case, when compromise events dominate over persuasion events, opinions are grouped around moderate values  $k = -1$  and  $k = 1$ , leading to centralization. Also, it was observed that stationary states of bi-polarization and centralization are unstable, given that a small opinion asymmetry is enough to drive the population to a fast consensus in one of the two extreme opinions. While these results correspond to the MF version of the M-model, the consequences of the competition between persuasion and compromise have not been explored in spatial or complex interaction topologies.

In this article we study the dynamics of the M-model on a two-dimensional ( $2D$ ) square lattice, for the simplest and non-trivial case  $M = 2$ . Our goal is to investigate the effects of the persuasion and compromise mechanisms in a population of agents with nearest-neighbor (short range) interactions, in contrast to the all-to-all interactions of the MF case. In particular, we aim to explore how the  $2D$  spatial topology affects the stability of the polarized and centralized states. We also aim to understand basic properties of the approach to extremist consensus.

The mechanisms of persuasion and compromise have been implemented in several works to model opinion formation in interacting populations. On the one hand, persuasion have recently been introduced in some agent-based models [15, 16, 17, 18]. For instance, persuasion was used in Refs. [15, 16] as a degree of a person's self-conviction where, in addition to the influence from others, a person takes into account its own opinion when making a decision. The authors in Ref. [17] introduced a model where each individual can have one of two opposite opinions or be undecided, and each of these three choices is determined by its persuasion or degree of conviction on the given issue, represented by a real number on a persuasion interval. Another work studied a model where the persuasion takes place between opposite-orientation agents [18]. On the other hand, the compromise process was initially studied in models with continuous opinions and interaction thresholds [19, 20], and the stability of the bimodal opinion distribution was tested under the influence of noise [21]. Some multistate voter models [22, 23, 24, 25] have incorporated a rule similar to compromise that uses a reinforcement mechanism by which agents switch orientation only after receiving multiple inputs of agents with opposite orientation. For instance, Castelló et al. [22] studied a three-state language model where each agent could either speak one of two possible languages (A or B) or be a bilingual AB. A monolingual A-agent can become bilingual AB by interacting with an agent that speaks the opposite language (B-agent or AB-agent). They investigated the ordering process of the system on regular lattices and small world networks, and the mean consensus time associated to each topology. A stability analysis of this model [26] revealed that the dominance of one language is enhanced by the connectivity of

the network, and that this effect is even stronger in lattices. More recently, Volovik and Redner [23] studied a voter model with four states, in which each agent can choose between two possible opinions and can additionally have two levels of commitment to the opinion (confident and unsure). A confident voter that interacts with an agent of a different opinion becomes less committed (unsure), but keeps its opinion. However, an unsure voter can change its opinion by interacting with an agent of a different opinion. In another work [24] Dall’Asta and Galla performed a numerical and analytical study of the coarsening properties of general voter models with many intermediate states on lattices [25], which have interaction rules similar to that of the works [22, 23] described above. They showed that the addition of intermediate states to the 2-state voter model (VM) [27] restores an effective surface tension. It is important to mention that all these models lack the mechanism of strengthening of opinions induced by the same-orientation interactions that characterizes the M-model.

The rest of the paper is organized as follows. In section 2 we describe the M-model on a  $2D$  square lattice. In section 3 we analyze the temporal evolution of the system and explore the coarsening dynamics in the regimes of bi-polarization and centralization. Results on the behavior of the mean consensus times are presented in section 4. In section 5 we investigate the dynamics of interfaces between opinion domains in the large persuasion limit. This study allows to derive an approximate expression for dependence of the mean consensus time with the system size, which explains the non-trivial scaling observed in the M-model and in general models with coarsening by surface tension. Finally, in section 6 we summarize and discuss our findings.

## 2. The M-model on a square lattice

We consider the opinion formation dynamics of the model proposed by La Rocca et al. [14] on a  $2D$  square lattice of  $N = L^2$  sites, where  $L$  is the linear size of the lattice. Each site is occupied by an agent who can interact with its four nearest neighbors, and can take one of four possible opinion states  $k = -2, -1, 1$  or  $2$  that represents its position on a political issue, from a negative extreme  $k = -2$  (a negative extremist) to a positive extreme  $k = 2$  (a positive extremist), taking moderate values  $k = -1, 1$  (a moderate). The sign of  $k$  and its absolute value  $|k|$  indicate the opinion orientation and its intensity, respectively. In a single time step of the dynamics of length  $\Delta t = 2/N$ , two nearest-neighbor agents  $i$  and  $j$  with respective states  $k_i$  and  $k_j$  are picked at random to interact. Then, their states are updated according to their opinion orientations (see Fig. 1):

- *Persuasion* [Figs. 1(a) and 1(b)]: If they have the same orientation ( $k_i, k_j > 0$  or  $k_i, k_j < 0$ ), then a persuasion event happens with probability  $p$ . An agent increases its intensity by one if it is a moderate ( $|k| = 1$ ), while it keeps its opinion if it is an extremist ( $|k| = 2$ ).
- *Compromise* [Figs. 1(c) and 1(d)]: If they have opposite orientations ( $k_i > 0$  and  $k_j < 0$  or  $k_i < 0$  and  $k_j > 0$ ), then a compromise event happens with probability

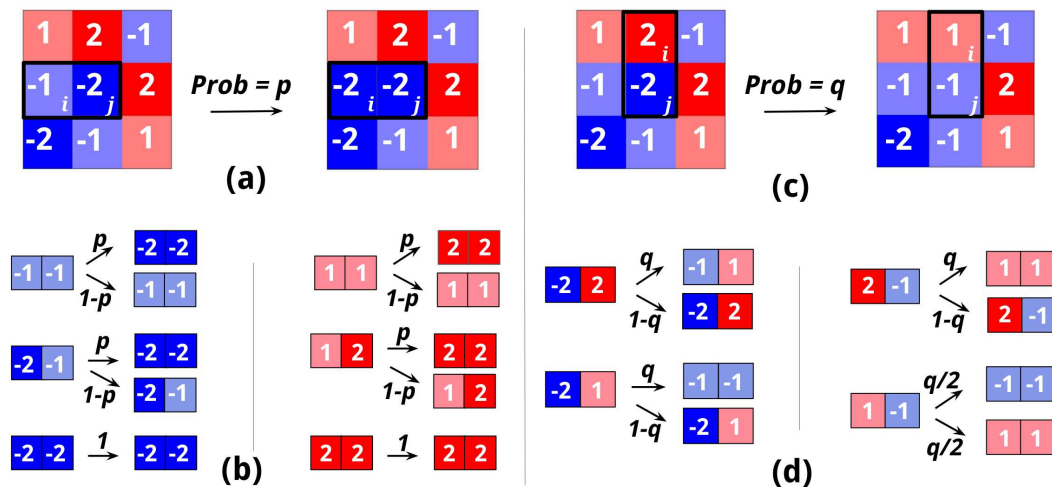


**Figure 1.** The two update events of the M-model on a square lattice. (a) and (b) Persuasion. In panel (a), a positive moderate agent  $i$  that has opinion  $k_i = -1$  becomes extremist ( $k_i = -1 \rightarrow k_i = -2$ ) with persuasion probability  $p$  by interacting with a nearest-neighbor agent  $j$  that has extreme opinion  $k_j = -2$ . Panel (b) shows all possible persuasion events in which two neighboring agents with the same opinion orientation reinforce their opinions and become extremists. (c) and (d) Compromise. In panel (c), two interacting neighbors with opposite and extreme opinions become moderate with probability  $q$  ( $k_i = 2 \rightarrow k_i = 1$  and  $k_j = -2 \rightarrow k_j = -1$ ). Panel (d) shows all possible compromise events in which two neighbors with opposite orientations become moderate.

$q$ . If both agents are extremists ( $|k_i| = |k_j| = 2$ ) they decrease their intensities by one. If one is an extremist and the other is a moderate  $|k| = 1$ , then the extremist decreases its intensity by one while the moderate switches orientation. If both agents are moderates one switches orientation at random.

We can think of persuasion and compromise as two competing mechanisms that shape the distribution of opinions in the population. While persuasive interactions make individuals adopt extreme opinions 2 and  $-2$  and lead to opinion bi-polarization, compromise contacts tend to moderate opinions, promoting a centralized opinion distribution around moderate values 1 and  $-1$ .

### 3. Coarsening dynamics

We started the analysis of the model by studying the time evolution of the number of agents in each state, which describes the system at the macroscopic level. For that, we run Monte Carlo simulations of the dynamics described in section 2 and measured the quantities  $x_k(t)$  ( $k = -2, -1, 1, 2$ ), defined as the fraction of agents in state  $k$  at time  $t$ , which are normalized at all times ( $\sum_k x_k(t) = 1$  for all  $t \geq 0$ ). Initially, each agent adopts one of the four possible states with equal probability  $1/4$ . The qualitative behavior of the system turns out to depend on the relative frequency between persuasion

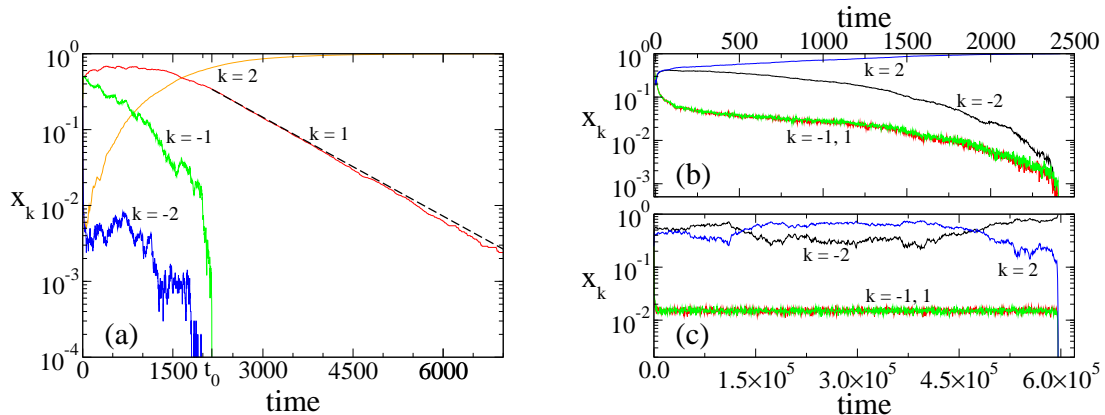


**Figure 2.** Time evolution of the densities  $x_k$  of agents in different opinion states  $k$  in single realizations of the dynamics, for a system of  $N = 10^4$  agents and two values of  $r = p/q$ . (a)  $x_k(t)$  for  $r = 10^{-3}$ . The dashed line is the expression  $0.34 e^{-r(t-2150)}$  from Eq. (2). Panels (b) and (c) show  $x_k(t)$  for  $r = 1/3$  in realizations of type 1 and type 2, respectively.

and compromise events, which is controlled by the ratio  $r \equiv p/q$  between persuasion and compromise probabilities. Therefore, for convenience we set  $p + q = 1.0$  [ $p = r/(1+r)$  and  $q = 1/(1+r)$ ] and analyzed the system as  $r$  is varied. In Fig. 2 we show the evolution of the densities  $x_k$  in single realizations of the dynamics for a system of size  $N = 10^4$ , and two different values of  $r$ .

In the realization with a very small  $r = 10^{-3}$  [Fig. 2(a)] compromise interactions are much more frequent than persuasive interactions ( $q \gg p$ ), driving most agents' opinions towards moderate values during an initial stage ( $t \lesssim 500$ ) in which  $x_1$  and  $x_{-1}$  are much larger than  $x_2$  and  $x_{-2}$ . This corresponds to a centralization of opinions. Then, at time  $t_0 = 2150$  negative states  $-1$  and  $-2$  disappear and the density  $x_1$  decays exponentially fast to zero, while  $x_2$  approaches exponentially fast to 1. Once  $x_2$  equals 1 the system cannot longer evolve (absorbing state), which in this case corresponds to a positive extremist opinion consensus. In a general case, the ultimate state of the system is always consensus in either extremist state, i.e., all agents with opinion 2 ( $x_2 = 1$ ) or all with opinion  $-2$  ( $x_{-2} = 1$ ). An insight into this exponential approach to consensus can be obtained within a mean-field (MF) approximation which assumes that every agent interacts with every other agent. This corresponds to the MF version of the M-model for small  $r$  studied in [14]. After time  $t_0$  only positive states 1 and 2 remain in the system ( $x_1(t) + x_2(t) = 1$ ), and thus the dynamics is only driven by persuasive events that slowly drive all agents to state 2 with a very small probability  $p = r/(1+r) \simeq r$  in the  $r \ll 1$  limit. Then, the mean change of  $x_1$  in a single time step of length  $\Delta t = 2/N$  is given by

$$\frac{dx_1}{dt} = \frac{\Delta x_1}{\Delta t} = -\frac{p x_1^2 \frac{2}{N}}{2/N} - \frac{p 2 x_1 x_2 \frac{1}{N}}{2/N} = -p x_1 \quad \text{for } t \geq t_0. \quad (1)$$

The first term of Eq. (1) describes the interaction between two state-1 agents that make



the transition to state 2 with probability  $p$ , while the second term accounts for the transition to state 2 of a state-1 agent that interacts with a state-2 agent. The solution of Eq. (1) is

$$x_1(t) = x_1(t_0) e^{-r(t-t_0)} \quad \text{for } t \geq t_0, \quad (2)$$

where we have used  $r$  as an approximate value for  $p$ . Expression Eq. (2) for  $x_1$  is plotted in Fig. 2(a) (dashed line) using  $r = 10^{-3}$  and the initial condition  $x_1(t_0 = 2150) \simeq 0.34$  extracted from the curve of  $x_1(t)$ . The good agreement with simulations shows that the dynamics on the lattice for small  $r$  is well described by the MF theory.

In the realizations with  $r = 1/3$  [Figs. 2(b) and 2(c)] persuasive interactions, which are more frequent than in the previous case but still less often than compromise interactions, seem enough to make most agents adopt extreme states 2 and  $-2$ , and thus  $x_2$  and  $x_{-2}$  are larger than  $x_1$  and  $x_{-1}$  for all times. This corresponds to a polarized state where the population of agents is divided in two groups of similar size that hold extreme and opposite opinions. We also observe that in the realization of panel (b) the system reaches consensus in extremist state 2 at time  $t \simeq 2400$ , while in the realization of panel (c) an extremist consensus in state  $-2$  is achieved in a much longer time  $t \simeq 6 \times 10^5$ . These examples correspond to two different types of realizations observed in simulations. In realizations of type 1 [panel (b)] the initial symmetry between positive and negative states is broken at early times and the system is quickly driven towards consensus, where the densities  $x_1$  and  $x_{-1}$  decay to zero and either  $x_2$  or  $x_{-2}$  approaches 1. In realizations of type 2 [panel (c)] the system falls in a long-lived metastable state where  $x_1$  and  $x_{-1}$  fluctuate around a stationary value for a very long time until they drop to zero together with  $x_2$ . This metastable state lasts for a much longer time than the one observed in the MF version of the model [14]. This means that the coexistence of opinions could be very stable when interactions are restricted to nearest-neighbors on a lattice, increasing the stability of the opinion bi-polarization.

In order to investigate the origin of the different behaviors described above we study the coarsening properties of the system by looking at the density of interfaces  $\rho$ , defined as the density of bonds between neighbors in different states [22, 24]. In Fig. 3 we show the time evolution of  $\rho$  in single realizations for  $r = 10^{-4}$  [panel (a)] and  $r = 1/3$  [panel (b)], together with snapshots of the lattice at different times and for each type of realization. We observe the formation of same-opinion domains with different characteristics. For  $r = 10^{-4}$  [Fig. 3(a)], the large frequency of compromise events as compared to persuasive events drives almost all agents towards moderate states, leading to the early formation of large domains composed by agents with states 1 or  $-1$ , with a few sparse extremists (down-left snapshot). During this stage, the dynamics at the interface between 1 and  $-1$  domains follows that of the VM. This explains the noisy shape of the interface that characterizes the coarsening without surface tension of the VM [28]. The domains slowly growth in size until almost all agents –except for a few extremists– adopt the same moderate state (state 1 in the snapshot), and  $\rho$  reaches a minimum. This corresponds to the beginning of the persuasive stage discussed

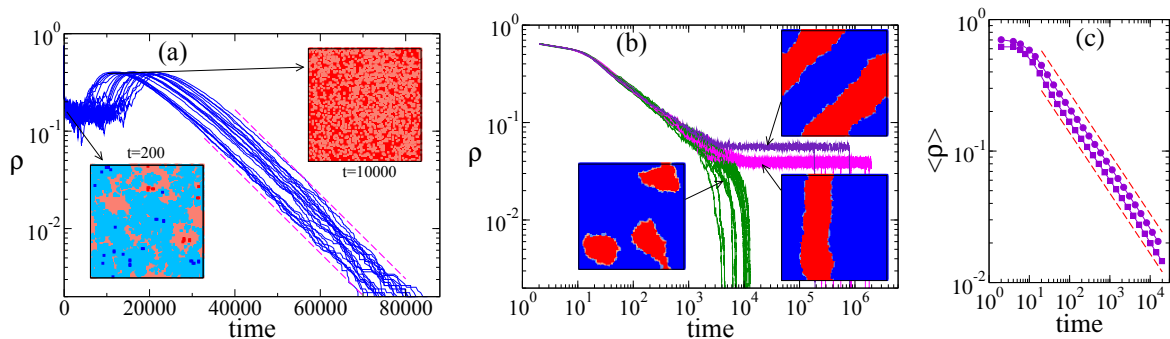


**Figure 3.** Time evolution of the interface density  $\rho$  in single realizations, for a system of size  $N = 10^4$  and  $r = 10^{-4}$  (a) and  $r = 1/3$  (b). The snapshots of the lattice show the spatial pattern of opinions at different times and for different realization types. Panel (a): the down-left snapshot corresponds to the centralization of opinions around moderate values  $k = -1$  and  $k = 1$ , while in the top-right snapshot all opinions are positive and driven by persuasion. Dashed lines have slope  $r = 10^{-4}$ . Panel (b): the down-left snapshot corresponds to realizations that reach a quick consensus by domain coarsening (type 1), while down-right and top-right snapshots represent realizations of type 2, where the system gets trapped in a long-lasting stripe state before reaching consensus. Panel (c): average interface density  $\langle \rho \rangle$  (circles) and average density of moderate states (squares) vs time on a system of size  $N = 300^2$ . The average was done over  $10^4$  realizations. Dashed lines have slope  $-0.46$ .

previously, during which moderate agents become extremists. The final relaxation to consensus follows the MF exponential decay  $\rho \simeq x_1(1 - x_1) \sim e^{-rt}$  from Eq. (2) (dashed lines). We note that this dynamics is very different from that observed in related multistate voter models [22, 24, 23], where agents with intermediate (moderate) states place themselves at the boundaries between extreme-state domains and form rather smooth interfaces. This last phenomenon happens for  $r = 1/3$  [Fig. 3(b)], where moderate states 1 and  $-1$  are located at the interface between 2 and  $-2$  domains. This is checked in Fig. 3(c) where we show the time evolution of the average value of  $\rho$  and the average density of moderate (intermediate) states  $x_1 + x_{-1}$ . We see that both  $\langle \rho \rangle$  and  $\langle x_1 + x_{-1} \rangle$  decay as  $t^{-0.46}$ , indicating that the interface dynamics is correlated with that of the moderate states. The behavior  $\langle \rho \rangle \sim t^{-0.46}$  is consistent with the algebraic coarsening found in voter models with intermediate states [22, 24]. As it was shown in [24], the addition of intermediate states to the 2-state VM changes the phase-ordering properties of the system, from a coarsening driven by interfacial noise observed in the VM to a coarsening driven by surface tension in models with one or many intermediate states. Also, the coarsening exponent 0.46 is compatible with the exponent 0.5 associated to the domain growth driven by curvature observed in kinetic Ising models [29, 30].

Another observation from Fig. 3(b) is related to the different types of realizations, whose interface dynamics explains the temporal behavior of the moderate densities  $x_1$  and  $x_{-1}$  observed in Figs. 2(b) and 2(c). The initial evolution of  $\rho$  in all realizations



follows the power-law decay described above, but then they split in two main groups. The group of short-lived realizations corresponds to Fig. 2(b), in which small domains shrink and disappear until one large extremist domain covers the entire lattice (down-left snapshot). The group of realizations that fall into a long-lived metastable state, which consists on either horizontal stripes or vertical stripes (down-right snapshot) or diagonal stripes (top-right snapshot), corresponds to Fig. 2(c). In these dynamical metastable states, the interface density  $\rho$  fluctuates around a stationary value until a finite-size fluctuation takes the system to one of the absorbing states ( $\rho = 0$ ). The long plateau observed in  $\rho$  shows that the polarized state is much more stable in lattices than in MF [14]. As we shall study in more detail in section 5, this behavior is due to the slow diffusion of the interfaces between these stripes, which eventually meet and annihilate and lead the system to consensus. Diagonal stripes are characterized by a stationary value of  $\rho$  that is approximately  $\sqrt{2}$  times larger than the corresponding value for horizontal or vertical stripes. It is also worth mentioning that, even though diagonal stripes were not reported in related models [22, 23, 31] probably because they are very unlikely to be formed (around 3 percent of the time in our simulations), we expect to see diagonal stripes in all these models with Ising-like coarsening [32].

#### 4. Consensus times

As we showed in section 3, the M-model has two absorbing states corresponding to the two extremist consensus. A magnitude of interest in these models is the mean time to reach opinion consensus  $\tau$ . In Fig. 4(a) we present results from numerical simulations of  $\tau$  as a function of  $r$  and three different lattice sizes  $N$ . Each data point corresponds to an average over  $10^4$  independent realizations with uniform initial condition. We see that  $\tau$  has a non-monotonic shape with  $r$ , taking very large values for small and large  $r$ . We also observe that  $\tau$  increases with  $N$  and that the increase is much faster for large  $r$ , which suggests two different scalings at both sides of the minimum. Indeed, panels (b) and (c) of Fig. 4 show the collapse of the data at small and large values of  $r$  when curves are rescaled by  $\ln N$  and  $N^{1.64}$ , respectively. The logarithmic scaling of  $\tau$  with  $N$  in the small  $r$  limit can be obtained from the behavior of the density  $x_1$  given by Eq. (2). We first note that the exponential decay of  $x_1$  with time holds for any  $r \ll 1$  and  $N$  (not shown), and that the time  $t_0(r, N)$  at which the persuasive stage begins varies with both  $r$  and  $N$ . To derive an expression for  $\tau$  we make two assumptions. First, we expect that the distribution of states at  $t_0(r, N)$  is peaked at  $k = 1$ , i e.,  $x_1(t_0) \simeq 1$  and  $x_2(t_0) \simeq 0$ . Indeed, we have checked that  $x_1(t_0)$  approaches 1.0 as  $r$  decreases ( $x_1(t_0) \simeq 0.34$  for  $r = 10^{-3}$  while  $x_1(t_0) \simeq 0.7$  for  $r = 10^{-4}$ ). Second, we assume that the consensus is reached when there is less than one agent in state 1, which leads to the condition  $x_1 = 1/N$  at  $\tau$ . Then, solving for  $\tau$  from the relation  $1/N \simeq e^{-r[t-t_0(r, N)]}$  we arrive to the approximation  $\tau \simeq t_0(r, N) + r^{-1} \ln N$ . The second term associated to the duration of the persuasive stage dominates in the small  $r$  limit and, therefore,  $\tau$  can be

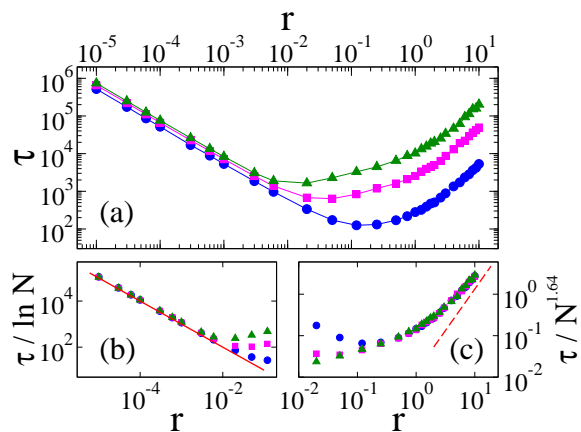


**Figure 4.** (a) Mean consensus time  $\tau$  as a function of  $r$  on a double logarithmic scale for lattice sizes  $N = 100$  (circles),  $N = 400$  (squares) and  $N = 900$  (triangles). Panels (b) and (c) show the data collapse for small and large  $r$ , respectively. The solid line in (b) is the analytical approximation  $\tau \simeq r^{-1} \ln N$  from Eq. (3), while the dashed line in (c) has slope 2.

approximated as

$$\tau \simeq \frac{\ln N}{r} \quad \text{for } r \ll 1. \quad (3)$$

We observe in Fig. 4(b) that the analytical expression Eq. (3) represented by a solid line has a good agreement with numerical data, showing the  $1/r$  divergence of  $\tau$  in the  $r \rightarrow 0$  limit.

The power-law behavior  $\tau \sim N^{1.64}$  used to collapse the data for large  $r$  [see Fig. 4(c)] was obtained by running simulations for  $r = 1/3$  and various system sizes. Results are shown in Fig. 6 with empty circles, where we also plot a solid line with slope 1.64 which serves as a guide to the eye, corresponding to the best fit of the data. The data points of Fig. 4(c) collapse into a single curve that seems to approach the quadratic behavior  $r^2$  as  $r$  becomes large (dashed line), which surprisingly agrees with that predicted by the MF expression  $\tau_{\text{MF}} \sim r^2 \ln N$  derived in [14]. However, this logarithmic increase of  $\tau_{\text{MF}}$  with  $N$  in MF is much slower than the non-linear increase  $\tau \sim N^{1.64}$  obtained in lattices. As consequence, the consensus in MF is much faster than in lattices.

As we explain below, long consensus times in lattices for large  $r$  are a consequence of the long-lived metastable states that characterize the realizations of type 2 discussed in section 3, which lead to the non-trivial scaling exponent 1.64. Indeed, the value of  $\tau$  obtained from simulations is the combination of two main types of realizations that have very different time scales. That are, realizations of type 1 where consensus is reached by domain coarsening, and realizations of type 2 in which consensus is reached by the diffusion of the two interfaces that define the stripe. To distinguish between type-1 and type-2 realizations we follow the method developed in [31, 22] and study the distribution of consensus times  $P(t)$ , from where the mean consensus time is calculated as  $\tau = \int_0^\infty t P(t) dt$ . This is equivalent to study the survival probability  $S(t)$  of single runs defined as the probability that a realization did not reach consensus up to time

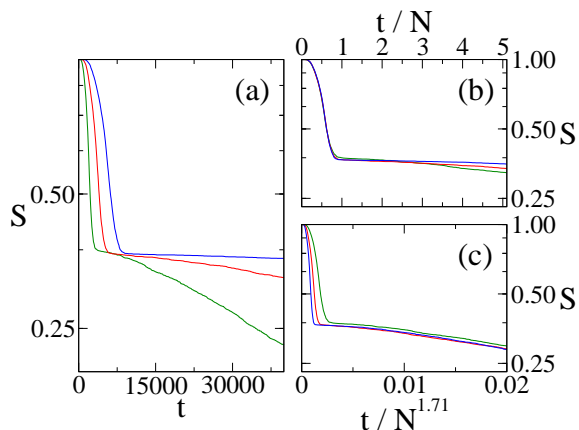


**Figure 5.** (a) Survival probability  $S$  vs time on a linear-log scale, for  $r = 1/3$  and system sizes  $N = 3600, 6400$  and  $10000$  (from bottom to top). The initial fast decay of  $S$  describes the domain coarsening, which has a mean lifetime proportional to  $N$  [panel (b)]. The long exponential tail of  $S$  decays with a time constant proportional to  $N^{1.71}$ , associated to the mean lifetime of type-2 realizations [panel (c)].

$t$ , which is related to  $P(t)$  by the expression  $S(t) = 1 - \int_0^t P(t) dt$ . The advantage of calculating  $S$  instead of  $P$  is that  $S$  has less fluctuations associated to the finite number of realizations. Figure 5(a) shows  $S$  vs time for  $r = 1/3$  and three system sizes. In agreement with results in related models [31, 22], curves are characterized by two time scales – a short time scale consistent with a fast decay to consensus, and a much longer time scale associated with an asymptotic exponential decay (the tail). The initial fast decay of  $S$  corresponds to the consensus induced by coarsening observed in type-1 realizations, while the exponential tail describes the consensus times of realizations that get trapped in a stripe metastable state (type-2 realizations). Then, the time  $t^*$  at which the exponential decay begins was taken as a reference to assign a type to a given realization. Realizations that reached consensus before (after)  $t^*$  were considered of type 1 (type 2). Using this criteria we estimated the time to reach consensus in each type of realization. In Fig. 6 we show that the mean consensus time scales as  $\tau_1 \sim N$  in type-1 realizations, while the scaling  $\tau_2 \sim N^{1.71}$  was found for type-2 realizations. The data collapse in panels (b) and (c) of Fig. 5 shows that  $\tau_1$  can be considered as the characteristic time scale associated to the fast initial decay of  $S$ , and that  $\tau_2$  is proportional to the time constant of the exponential decay. We have also calculated the probability that a realization reaches the metastable state as the fraction of type-2 realizations over  $10^3$  independent runs, which gave the approximate mean value 0.34 in the size range  $400 \leq N \leq 10000$ , with a very slow decrease as  $N$  increases. The indirect estimation of the mean consensus time as the combination of the two realization types

$$\tau \simeq 0.66 \tau_1 + 0.34 \tau_2 \quad (4)$$

is plotted in the inset of Fig. 6 (solid diamonds), where we observe a good agreement with the value of  $\tau$  calculated over all realizations (empty circles). Therefore, the approximate scaling  $\tau \sim N^{1.64}$  observed in simulations can be explained as the result of the linear

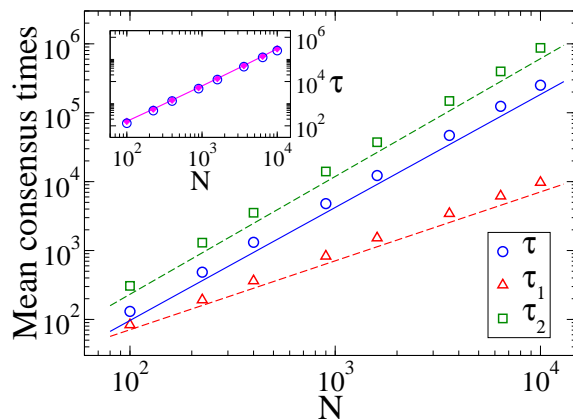


**Figure 6.** Mean consensus times  $\tau$ ,  $\tau_1$  and  $\tau_2$  vs system size  $N$  on a log-log scale for  $r = 1/3$ .  $\tau$  is the average over all  $10^4$  realizations, while  $\tau_1$  and  $\tau_2$  correspond to the average values over realizations of type 1 and type 2, respectively. Straight lines have slopes 1.71, 1.64 and 1.0 (from top to bottom). Inset: the estimation of the mean consensus time as the linear combination  $0.66\tau_1 + 0.34\tau_2$  (diamonds) of both realization types is compared to  $\tau$  (circles).

combination of the power-law behaviors  $\tau_1 \sim N$  and  $\tau_2 \sim N^{1.71}$ . Since  $\tau_2$  becomes much larger than  $\tau_1$  as  $N$  increases –by a factor of 10 (100) for  $N = 400$  ( $10^4$ ), we expect that the effective exponent 1.64 of  $\tau$  will approach the exponent of  $\tau_2$  as  $N$  increases. In the next section we provide an explanation of the non-trivial exponent 1.71 by studying the dynamics of stripes in detail.

## 5. The dynamics of stripes towards consensus

In section 4 we showed that the mean consensus time for  $r = 1/3$  scales as  $\tau \sim N^{1.64}$  with the system size  $N$ . As discussed previously, this scaling is mainly due to the existence of metastable states that survive for very long times, in which the system exhibits a stripe-like pattern. It is important to mention that very similar scaling laws for the consensus time with system size,  $\tau \sim N^\nu$ , were already reported in the literature in related works in lattices [31, 22, 23]. For instance, in the Majority Rule (MR) model introduced in [31] the authors found  $\nu = 1.7$ , while in the bilinguals model studied in [22] an exponent  $\nu = 1.8$  was obtained, and also a similar exponent was observed in the confident VM investigated in [23], whose exact value was not reported. What all these models have in common with the M-model on a lattice is the existence of stripe states with a probability around  $1/3$  when the system starts from random initial conditions, and an ultimate consensus state that is absorbing. Despite that these models differ in the number of opinion states (2 states in MR model, 3 states in the bilinguals model, 4 states in the confident VM, and 4 or more states in the M-model), their microscopic rules induce a coarsening dynamics that is driven by surface tension, which can lead to the formation of horizontal, vertical or diagonal stripes in square lattices, as it is known to happen in Ising-like systems [32]. Therefore, it seems that the dynamics of stripes is

the fundamental mechanism that determines the consensus times in lattice models with coarsening by surface tension and frozen consensus states, leading to the scaling  $\tau \sim N^\nu$  (with  $1.64 \leq \nu \leq 1.8$ ) reported in the works mentioned above. As far as we know, there is no yet a satisfying explanation for the behavior of  $\tau$  with  $N$ . Some attempts to obtain the exponent  $\nu$  were developed in [31] and [23], which arrived to the approximate value  $\nu = 1.5$  that is far from the exponent obtained from numerical simulations of the respective models,  $\nu = 1.7$  and  $\nu = 1.8$ .

In this section we propose an approach that gives an insight into the dynamics of the system towards consensus and provides a value of  $\nu$  in good agreement with simulations. Equation (4) shows that the mean consensus time has a linear contribution ( $\tau_1 \sim N$ ) that corresponds to short-lived realizations (type 1) and a non-linear term ( $\tau_2 \sim N^{1.71}$ ) corresponding to long-lived realizations (type 2). Given that  $\tau_1$  is much smaller than  $\tau_2$  for the explored range of  $N$  (see Fig. 6), we can assume that  $\tau$  is mainly determined by the long-lasting realizations that fall into a stripe state (type-2 realizations). The evolution of a typical type-2 realization consists on two different stages, as we can see from the evolution of  $\rho$  in Fig. 3(b). The initial stage is characterized by the dynamics of domain coarsening where  $\rho$  exhibits a power-law decay up to a time  $t \simeq 10^4$ . Then, the system falls into a striped metastable state where  $\rho$  stays nearly constant until consensus is reached at time  $t \simeq 2 \times 10^6$ . Therefore, we see that the consensus time is greatly controlled by the duration of this stripe stage, given that it is much longer than the initial coarsening stage.

To studied the dynamics of stripes we prepared the system in an initial condition that consisted on two vertical stripes of width  $L/2$  each, as we see in Fig. 7(a-I). Figure 7(a) shows a typical evolution of the stripes in a single realization, where we combined both opinions of a given orientation into a single color to make the interfaces look more clear to the eyes ( $-1$  and  $-2$  in blue,  $1$  and  $2$  in red). The interfaces that separate the stripes freely diffuse in the direction perpendicular to the interfaces [Fig. 7(a-II)] until they meet and annihilate each other, cutting one stripe in two [Fig. 7(a-III)]. Then, during the last stage, the resulting domain quickly shrinks [Fig. 7(a-IV)] and dissappear, and the system reaches consensus. As this last stage is much shorter than the diffusive stage, the mean consensus time starting from a stripe initial state, called  $\tau_s$ , can be approximated as the mean time required for the two interfaces to meet and break, which we call the “mean breaking time”  $\tau_b$ . In Fig. 7(b) we verify that  $\tau_b$  (squares) is indeed very similar to  $\tau_s$  (up triangles). We also see that  $\tau_b$  is similar to the mean consensus time  $\tau_2$  of type-2 realizations starting from a random initial condition (left triangles), as we suggested previously. Then, using Eq. (4) we find that  $\tau$  can be approximated as

$$\tau \simeq 0.34 \tau_b, \tag{5}$$

represented by diamonds in Fig. 7(b). Based on this result, we derive in subsection 5.1 an analytical approximation for the dependence of  $\tau_b$  with  $L$  using the diffusion properties of the interfaces, and in subsection 5.2 we improve this approximation by

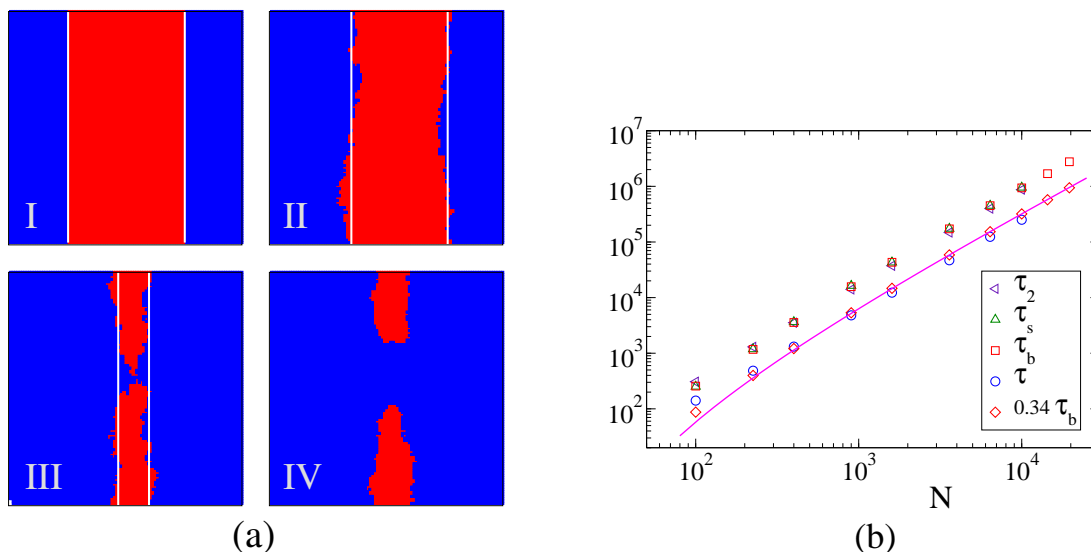


**Figure 7.** (a) Snapshots of a  $100 \times 100$  square lattice at four different times, showing the evolution of same-opinion-orientation stripes in a single realization (negative opinions  $-1$  and  $-2$  in blue and positive opinions  $1$  and  $2$  in red). Vertical straight lines denote the position of the stripe interfaces. (b) We compare the mean consensus time of type-2 (stripe) realizations starting from a random initial condition  $\tau_2$  (left triangles), with the mean consensus time  $\tau_s$  (up triangles) and the mean interface breaking time  $\tau_b$  (squares) starting from the striped configuration showed in snapshot I of panel (a). We also compare the mean consensus time  $\tau$  (circles) with the estimation  $0.34 \tau_b$  (diamonds). The solid line is the analytical approximation from Eq. (11).

incorporating the roughness properties of the interfaces.

### 5.1. Estimation of $\tau_b$ considering two diffusive point-like particles

To study the dynamics of the interfaces we start by defining the position  $x_i(t)$  of interface  $i$  ( $i = 1, 2$ ) at a given time  $t$  as the mean value of the interface positions  $x_{i,y}(t)$  at height  $y$  [see Fig. 8(a)]

$$x_i(t) = \frac{1}{L} \sum_{y=1}^L x_{i,y}(t). \quad (6)$$

Then, we can interpret  $x_1$  and  $x_2$  as the respective positions of two independent point-like particles that diffuse in an interval  $[1, L]$  with periodic boundary conditions, which they annihilate when they meet. This equivalence was proposed by Chen and Redner in the MR model [31], and also used later by Volovik and Redner in the confident VM [23]. We have checked that particle 1 (and also particle 2) moves diffusively by measuring the time evolution of the variance of  $x_1$ ,  $\sigma^2(t) = \langle x_1^2 \rangle(t) - \langle x_1 \rangle^2(t)$ , where averages were done over  $10^4$  independent realizations. We found that  $\sigma^2(t)$  increases linearly with time for various linear sizes  $L$  and that the diffusion coefficient  $D_L$ , calculated from the relation  $\sigma^2(t) = 2 D_L t$  of a diffusive process, decays as  $1/L$  (plots not shown). Indeed,



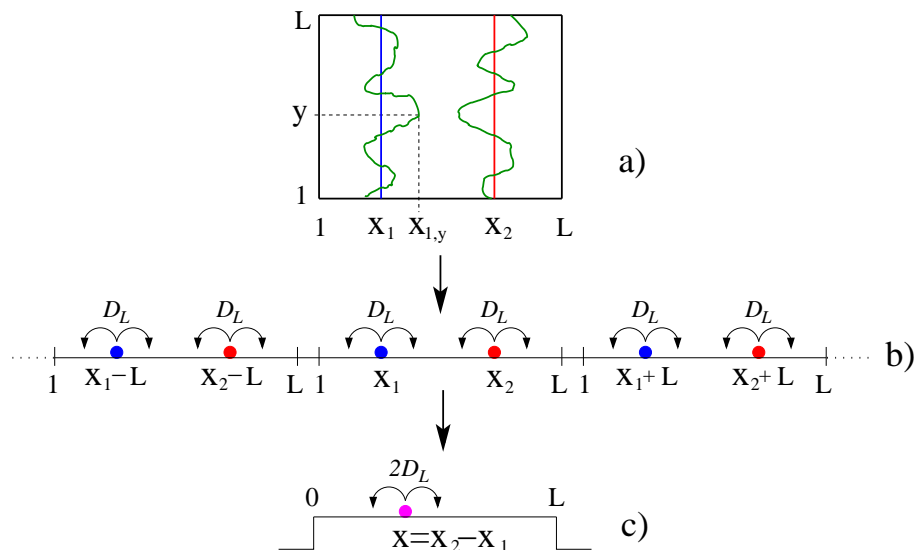


**Figure 8.** Illustration of the mapping of the stripe interface dynamics to the problem of two diffusive point-like particles in an interval  $[1, L]$  with periodic boundary conditions. a) Vertical lines indicate the positions  $x_1$  and  $x_2$  of the interfaces, denoted by circles (particles) in panel b). b) The system is replicated in the entire  $1D$  space, where the particles diffuse freely with no boundary constraints. c) The equivalent particle with position  $x = x_2 - x_1$  diffuses in the interval  $[0, L]$  with absorbing boundaries at the ends. The diffusion coefficient  $2D_L$  is twice as that of particles in panel a).

we observed that all curves collapse when the  $y$ -axis is rescaled by  $L$ , obtaining the approximate relation

$$D_L \simeq \frac{d}{L}, \quad (7)$$

with  $d = 0.04$ . An estimation of this scaling relation was developed in [31, 23] by assuming that each point at the interface  $x_{i,y}$  behaves as an independent random walker [33, 34] that jumps one site to the right or left with equal probabilities. Then,  $\sqrt{D_L}$  should be proportional to the mean displacement of the interface's position  $x_1$  in a time interval  $\Delta t = 1$ , which scales with the number of walkers  $L$  as  $\sqrt{L}/L = L^{-1/2}$ , thus  $D_L \sim 1/L$ .

We can now approximate the mean interface breaking time  $\tau_b$  as the mean time the particles take to meet in the  $[1, L]$  interval, when their initial positions are a distance  $L/2$  apart. Given to the periodic character of the interval's boundaries, it proves useful to consider an equivalent system that is obtained by replicating the interval and particles in the one-dimensional ( $1D$ ) space [see Fig. 8(b)], where particles can freely diffuse in the entire  $1D$  space without boundary constraints. In this replicated system, particle 1 moves always between particle 2-left and particle 2 ( $x_2 - L \leq x_1 \leq x_2$ ) until it annihilates with one of these two particles ( $x_1 = x_2 - L$  or  $x_1 = x_2$ ). Thus, the difference  $x \equiv x_2 - x_1$  can be seen as the position of an equivalent particle that diffuses in the interval  $[0, L]$  with absorbing boundaries at  $x = 0$  and  $x = L$  [see Fig. 8(c)]. Then, the problem is

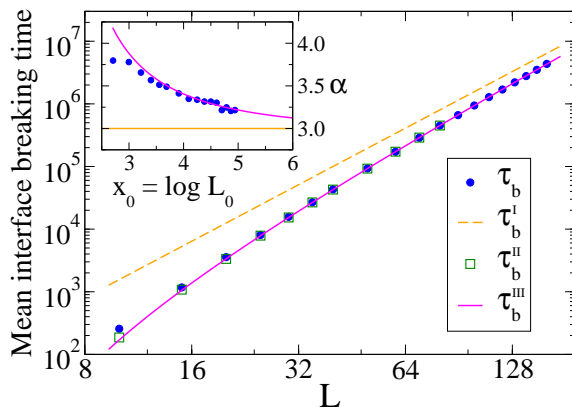


**Figure 9.** Mean interface breaking time vs lattice side  $L$  on a log-log scale starting from the stripe initial condition of Fig. 7(a-I). We compare simulation results ( $\tau_b$ , filled circles) with the following approximate expressions:  $\tau_b^I$  (dashed line) from Eq. (8),  $\tau_b^{II}$  (empty squares) from Eq. (9) and  $\tau_b^{III}$  (solid line) from Eq. (10). Inset: Circles correspond to the local slope of the  $\tau_b$  vs  $L$  curve on a log-log scale calculated from the data points of the main figure, while the solid line is the analytic approximation Eq. (14).

reduced to the escape of a particle with diffusion  $2D_L$  (twice of that of particles 1 and 2) from an interval  $[0, L]$  starting from a position  $x = L/2$ , whose exact expression for the mean exit time is known to be  $L^2/16D_L$  (see for instance [35]). After replacing the expression Eq. (7) for  $D_L$  we obtain

$$\tau_b^I = \frac{L^3}{16d}, \quad (8)$$

where the superindex I in  $\tau_b^I$  is used to indicate a first-order approximation for  $\tau_b$  (see next subsection for higher-order approximations). In Fig. 9 we compare the expression Eq. (8) for  $\tau_b^I$  (dashed line) with the value of  $\tau_b$  obtained from numerical simulations (circles). Even though we see that  $\tau_b^I$  is a reasonable approximation of  $\tau_b$ , it overestimates  $\tau_b$  for all simulated values of  $L$ . However, we shall show later that  $\tau_b^I$  asymptotically approaches  $\tau_b$  in the  $L \rightarrow \infty$  limit. This observation was already reported in [31, 23] together with the approximate scaling  $\tau \sim L^3 = N^{3/2}$ .

### 5.2. Estimation of $\tau_b$ considering two diffusive rod-like particles

The meeting time  $\tau_b^I$  can be considered as a first approximation for  $\tau_b$ , where it is assumed that stripes' interfaces break when their positions become exactly the same ( $x_1 = x_2$ ). However, this approximation neglects the roughness of each interface, which plays an important role in the breaking dynamics as we shall see. A more refined approximation that takes into account the width of the interfaces considers that, in a given realization, the interfaces break when they are located at some distance  $\Delta x^b = |x_2^b - x_1^b| > 0$  apart [see Fig. 10(a)], where  $x_1^b$  and  $x_2^b$  are the respective interfaces' positions at the breaking time. The idea behind this argument is that the breaking happens when the interfaces touch by the first time at some point  $y$  that depends on the specific roughness of the

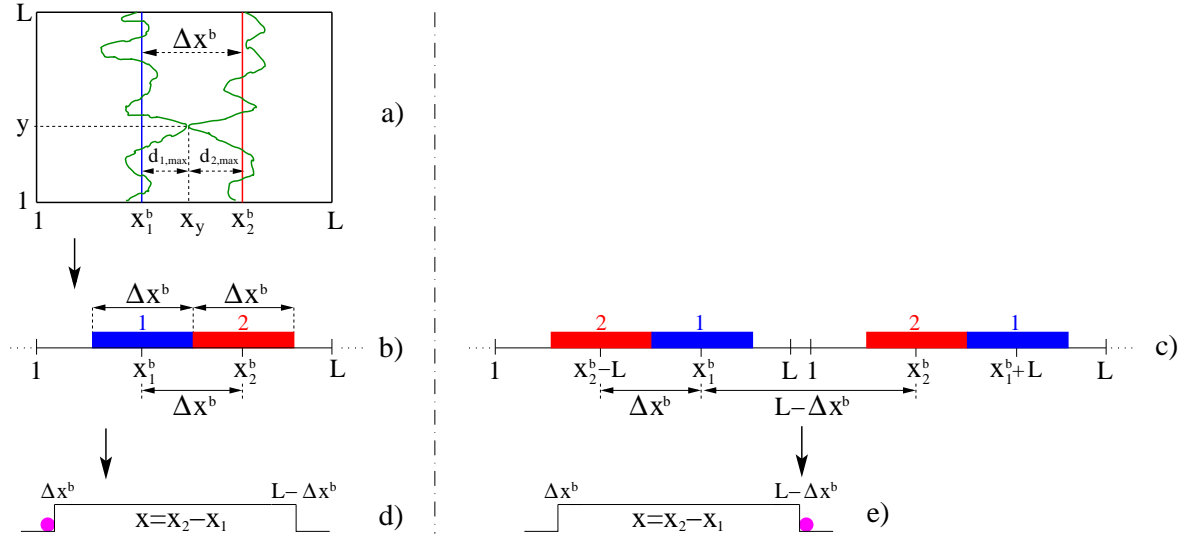


**Figure 10.** a) The stripe interfaces break when they are a distance  $\Delta x^b$  apart and they touch at a point  $y$  by the first time. b) and c) The interfaces are mapped to diffusive rod-like particles in the replicated 1D space that annihilate each other when they collide. d) and e) The equivalent point-like particle with position  $x = x_2 - x_1$  diffuses in the interval  $[\Delta x^b, L - \Delta x^b]$  with absorbing boundaries at the ends.

interfaces at that moment, as we see in Fig. 10(a). Therefore, each interface can be better described by a diffusive rod-like particle of length  $\Delta x^b$  that represents the interfaces' width at the breaking moment [see Fig. 10(b)]. These two rods diffuse until they collide and annihilate in one of the two possible ways shown in panels b) and c) of Fig. 10. In the replicated system, the center of rod 1 moves between positions  $x_1 = x_2 - \Delta x^b$  [panel b)] and  $x_1 = x_2 - L + \Delta x^b$  [panel c)], and thus the difference  $x = x_2 - x_1$  between the rods' centers describes the position of a point-like particle that moves in the interval  $[\Delta x^b, L - \Delta x^b]$  of reduced length  $L - 2\Delta x^b$  [panels (d) and (e)].

If we take the average value of  $\Delta x^b$  over many realizations of the dynamics,  $\langle \Delta x^b \rangle$ , as the effective distance between the interfaces when they touch by the first time, the problem can be reduced to the escape of a particle from an interval of “effective length”  $\bar{L} = L - 2\langle \Delta x^b \rangle$ . Then, the mean escape time is  $\bar{L}^2/16 D_L$  or, replacing the above expression for  $\bar{L}$  and Eq. (7) for  $D_L$ , is

$$\tau_b^{\text{II}} = \frac{(1 - 2\langle \Delta x^b \rangle L^{-1})^2 L^3}{16 d}. \quad (9)$$

Equation (9) represents a second approximation that incorporates the average distance between interfaces when they meet. To test Eq. (9) we run simulations and measured the average interface distance  $\langle \Delta x^b \rangle$  for several values of  $L$  [squares in Fig. 11(a)]. The interface breaking moment of a given realization was taken as the time for which all sites of at least one lattice row have either state 2 or  $-2$  by the first time. Empty squares in Fig. 9 represent the estimation  $\tau_b^{\text{II}}$  of  $\tau_b$  obtained by plugging the numerical value of  $\langle \Delta x^b \rangle$  into Eq. (9), which is in good agreement with simulation results (filled circles) for  $L \geq 15$ . This shows that the roughness of the interfaces plays a very important role in

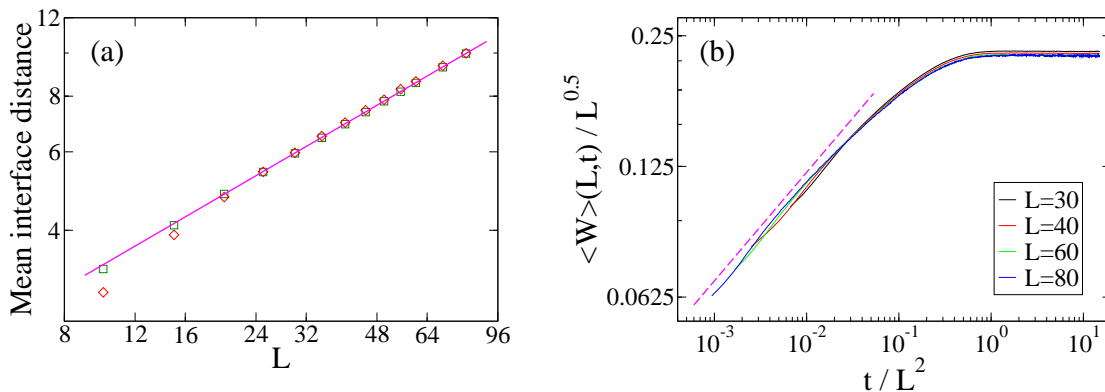


**Figure 11.** a) Average distance between interfaces when they break  $\langle \Delta x^b \rangle$  (squares) and average maximum interface deviation  $2\langle d_{max} \rangle$  (diamonds) as a function of  $L$ . The solid line is the best power-law fit  $L^{0.525}$  to  $\langle \Delta x^b \rangle$ . (b) Growth of the average interface width  $\langle W \rangle$  with time. The width and the time were rescaled by  $L^{0.5}$  and  $L^2$ , respectively, to obtain a data collapse for the linear sizes indicated in the legend. The dashed line indicates the initial power law growth  $t^{0.25}$ .

the breaking dynamics, leading to large deviations of  $\tau_b$  from the  $L^3$  scaling law (dashed line in Fig. 9) as  $L$  decreases. These deviations, which become very visible for low  $L$ , are captured rather well by the prefactor  $(1 - 2\langle \Delta x^b \rangle / L)^2$  of  $\tau_b^{\text{II}}$  in Eq. (9). We see in Fig. 11(a) that  $\langle \Delta x^b \rangle$  grows with  $L$  as  $L^{0.525}$  (solid line), and thus the ratio  $\langle \Delta x^b \rangle / L$  vanishes as  $L$  increases, leading to the expression Eq. (8) for  $\tau_b^{\text{I}}$  and confirming the hypothesis that Eq. (8) is correct in the  $L \rightarrow \infty$  limit. As we show in Appendix A, the exponent 0.525 is related to the *roughness exponent*  $\alpha \simeq 0.5$  associated to the saturation value of the interfaces' width. An interesting insight from Eq. (9) is that a pure power law  $\tau_b^{\text{II}} \sim L^{2\nu} = N^\nu$  is never obtained for a finite value of  $L$ . Instead, the correction factor  $(1 - 2\langle \Delta x^b \rangle / L)^2$  introduces a downward curvature in the  $\tau_b^{\text{II}}$  vs  $L$  curve on a double logarithmic scale, which decreases with  $L$  and becomes very small for  $L \gtrsim 40$  (see Fig. 9). As a result, the data can be well fitted by a power law function of  $N$  with an effective exponent  $\nu > 1.5$ , as those shown in Fig. 6 for  $\tau$  and  $\tau_2$ .

By plugging the power-law approximation  $\langle \Delta x^b \rangle \simeq L^{0.525}$  into Eq. (9) we obtain the following approximate expression for the mean breaking time:

$$\tau_b^{\text{III}} = \frac{(1 - 2L^{-0.475})^2 L^3}{16d}. \quad (10)$$

As we can see in Fig. 9, Eq. (10) represented by a solid line fits the numerical data (filled circles) very well for  $L \gtrsim 15$ . Finally, using Eq. (5) we arrive to the approximate expression

$$\tau \simeq \frac{0.34 (1 - 2N^{-0.2375})^2 N^{1.5}}{16d}. \quad (11)$$

for the mean consensus time. Equation (11) is plotted by a solid line in Fig. 7(b). We see that, even though there are some discrepancies with numerical results (circles), Eq. (11)

captures rather well the behavior of  $\tau$  with the system size for almost the entire range of  $N$  values.

We can now exploit the approximate functional form of  $\tau_b$  given by Eq. (10) to analyze the scaling of  $\tau_b$  for a wide range of  $L$ . The factor  $L^{-0.475}$  introduces a downward curvature in  $\tau_b^{\text{III}}$ —when plotted in log-log scale—that vanishes as  $L$  increases. Therefore, we can approximate the shape of  $\tau_b^{\text{III}}$  around a given value  $L_0$  as a power law of  $L$  (see Appendix B for calculation details)

$$\tau_b^{\text{III}}(L, L_0) \simeq A(L_0) L^{\alpha(L_0)}, \quad (12)$$

where

$$A(L_0) = \frac{1}{16d} (1 - 2L_0^{-0.475})^2 L_0^{\frac{1.9}{(2-L_0^{0.475})}} \quad \text{and} \quad (13)$$

$$\alpha(L_0) = 3 + \frac{1.9}{(L_0^{0.475} - 2)}. \quad (14)$$

We can check that in the thermodynamic limit  $L_0 \rightarrow \infty$  the exponent  $\alpha(L_0)$  approaches the value 3.0 as previously suggested, while  $A(L_0)$  approaches  $1/(16d)$ , recovering the approximation  $\tau_b^{\text{I}} \simeq L^3/(16d)$  from Eq. (8). The exponent  $\alpha(L_0)$  from Eq. (14), which measures the slope of the  $\log[\tau_b^{\text{III}}(L)]$  vs  $\log(L)$  curve at some point  $\log(L_0)$ , is plotted by a solid line in the inset of Fig. (9) and compared to the numerical value (filled circles) obtained by calculating the local slope of the  $\tau_b$  data points from the main figure. We can see that the slope decreases very slowly with  $L_0$ , and thus for the values of  $L$  measured in simulations  $\alpha$  stays nearly constant and can be approximated by a clean power law. Then, we can use Eq. (14) to approximate the mean breaking time as  $\tau_b \sim L^\alpha = N^{\alpha/2}$  in the range of system sizes used in simulations, and compare  $\alpha$  with the numerical exponents obtained from Fig. 6 by fitting the numerical data with a power law. For instance, the slope at  $N = 2000$  ( $L \simeq 45$ ) from Eq. (14) is  $\alpha/2 \simeq 1.73$ , which agrees quite well with the numerical slope 1.71 for  $\tau_2$  in the range  $4 \times 10^2 \leq N \leq 10^4$ . The theoretical value  $\alpha/2$  is also a fair approximation of the numerical exponent 1.64 obtained from the  $\tau$  vs  $N$  data (only 5.5% off), even though we expect that this approximation improves for larger values of  $N$ . Finally, we also note that it turns very difficult to reach a slope close to 1.5 in simulations of the model, because of the very slow decrease of  $\alpha$  with  $L_0$ . For instance, to achieve a slope smaller than 1.545 (less than 3% difference with 1.5) Eq. (14) predicts that we would need to run simulations in systems with linear dimension  $L \gtrsim 750$ , whose consensus times are of order  $\tau \sim 10^9$  (Eq. 10), which is almost impossible to achieve in reasonable computation times.

## 6. Summary and conclusions

We studied an agent-based model on a  $2D$  lattice that explores the competition between persuasion and compromise in opinion formation. We found that nearest-neighbor interactions between agents induce a very rich domain coarsening dynamics, which plays a fundamental role in the evolution of the system and the approach to consensus.

The properties of the coarsening strongly depend on the relative frequency between persuasion and compromise events, measured by the ratio  $r = p/q$  between persuasion and compromise interaction probabilities. When the compromise process dominates over the persuasion process the dynamics is akin to that of the VM during an initial short transient, in which domains are formed by moderate agents and the coarsening is without surface tension. This is associated to a centralized opinion state where most agents adopt moderate opinion values. Domain growth eventually leads to a state where all agents have the same opinion orientation (positive or negative). Then, moderate agents start to become extremists and the system displays a slow exponential approach to consensus in an extreme opinion that is achieved in a time that scales as  $r^{-1} \ln N$  with the population size  $N$ . In the opposite case scenario where persuasion dominates over compromise, the coarsening is driven by surface tension and moderate agents are located at the interface between domains formed by extremists. This corresponds to a polarized opinion state in which the population is divided into two groups that adopt extreme and opposite opinions (positive and negative). The final approach to consensus can be very long if the system falls into a striped metastable configuration, where the two interfaces that define a stripe diffuse until they meet and annihilate. The mean consensus time of this type of realizations scales as  $N^{1.71}$ . When the average is done over all realizations, which include short-lived realizations with a lifetime that scales as  $N$ , the scaling of the overall mean consensus time is  $\tau \sim N^\nu$ , with  $\nu = 1.64$ .

An insight into the approach towards consensus of striped configurations was obtained by mapping the dynamics of stripes into the problem of two rods that freely diffuse in  $1D$  and annihilate when they collide by the first time. This method takes into account the width of stripe interfaces, which becomes relevant when interfaces meet and break. An analytical estimation of the mean collision time using known results on first-passage problems allowed to obtain the approximate expression Eq. (10) for the mean lifetime of stripes, which is in good agreement with results from simulations of the model. Also, Eq. (11) for the mean consensus time shows that the scaling  $\tau \sim N^\nu$  is an approximation obtained by fitting with a power-law the numerical data over a finite range of  $N$ , given that the effective exponent  $\nu$  around a given  $N$  decreases and approaches the value 1.5 in the thermodynamic limit ( $N \rightarrow \infty$ ). These results show that analytical deviations from the scaling exponent  $\nu = 1.5$ , obtained by assuming that interfaces behave as point-like particles, are due to the roughness of the interfaces.

In summary, the  $2D$  spatial topology of interactions has a large impact on the behavior of the M-model respect to the MF case. Opinion bi-polarization is much more stable in lattices than in MF, due to the existence of long-lived metastable states with a spatial pattern of opinions that consists on two stripes composed by both types of extremists. This dynamics leads to consensus times in lattices that are much longer than those obtained in a MF setup. The width of the interfaces between stripe domains plays an important role in the dynamics close to consensus, when interfaces are about to annihilate each other. Taking into account the scaling properties of the interface width allows to derive an expression for the behavior of the mean consensus time



with the system size, in good agreement with simulations. This expression provides an explanation for the non-trivial numerical exponent  $\nu = 1.64$ , and also for similar exponents observed in related models where consensus is reached by curvature driven coarsening. Another observation is that the bi-polarization is found for  $p > q$  in MF, while in lattices is found for much lower values of persuasion, approximately for  $p > q/3$ . Therefore, a small level of homophily is enough to induce bi-polarization in a population that interacts in lattices. Thus, the lattice topology seem to intensify the effect of homophily and PAT on the emergence of bi-polarization. This result resembles that obtained in the Schelling model for racial segregation [36], where even a small preference to have neighbors of the same race on a lattice is able to induce a large spatial segregation of the population into same-race domains.

It would be worthwhile to study the dynamics of the M-model on complex networks of different kinds, which are more realistic descriptions of the topology of social interactions among people. It would also be interesting to investigate the role of the network connectivity in the propagation and ultimate dominance of an extreme opinion [26]. Finally, a natural extension of the model would include variations of the persuasion and/or compromise rules that could enhance bi-polarization in lattices or in general topologies.

## Acknowledgments

We would like to thank Gabriel Baglietto for helpful discussions. We also acknowledge financial support from CONICET (PIP 0443/2014).

## Appendix A. Analysis of the mean interface breaking distance $\langle \Delta x^b \rangle$

We can gain an insight into the scaling  $\langle \Delta x^b \rangle \simeq L^{0.525}$  by relating the distance between interfaces at the breaking moment with the properties of the interface roughness, as we illustrate in Fig. 10(a). More precisely, the interfaces touch at a high  $y$  ( $x_{1,y} = x_{2,y} = x_y$ ) where the respective interface deviations from  $x_1$  and  $x_2$  reach their maximum values  $d_{1,max} = |x_y - x_1^b|$  and  $d_{2,max} = |x_y - x_2^b|$ . Therefore, the distance between interfaces can be approximated as  $\Delta x^b \simeq d_{1,max} + d_{2,max}$ . Given that the high  $y$  of the touching point varies among realizations, we calculated the average value of the maximum deviation  $\langle d_{max} \rangle$  at both sides of each interface over many realizations of the dynamics. Results are shown in Fig. 11(a) (diamonds). We see that  $2 \langle d_{max} \rangle$  agrees very well with  $\langle \Delta x^b \rangle$  for  $L \gtrsim 20$ , and that follows the power-law scaling  $\langle d_{max} \rangle \sim L^{0.525}$  (solid line). We speculate that this scaling is related to the scaling properties of the width of the interfaces, defined as the standard deviation of the interface positions  $x_{i,y}$  along the  $y$ -axis [37, 38]

$$W_i = \left[ \frac{1}{L} \sum_{y=1}^L x_{i,y}^2 - \left( \frac{1}{L} \sum_{y=1}^L x_{i,y} \right)^2 \right]^{1/2} = \left[ \frac{1}{L} \sum_{y=1}^L (x_{i,y} - x_i)^2 \right]^{1/2}. \quad (\text{A.1})$$

The time evolution of the average interface width calculate over many realizations  $\langle W \rangle$  [see Fig. 11(b)] has an initial stage in which  $\langle W \rangle$  grows as  $t^\beta$ , followed by a second stage where  $\langle W \rangle$  reaches a saturation value (plateau) that increases with  $L$  as  $\langle W \rangle_{\text{sat}}(L) \sim L^\alpha$ , where  $\alpha \simeq 0.5$  is the *roughness exponent* and  $\beta \simeq 0.25$  is the *growth exponent*. These exponents are consistent with those of the Edwards-Wilkinson universality class of surface growth [38]. Indeed, by an appropriate rescaling of the  $x$  and  $y$  axis the data can be collapsed into a single function [Fig. 11(b)] showing that the interface growth obeys the Family-Vicsek scaling relation  $\langle W \rangle(L, t) = L^\alpha f(t/L^z)$  with  $z = \alpha/\beta \simeq 2$ , and  $f(x) \sim x^\beta$  for  $x \ll 1$  and  $f(x) = \text{constant} \simeq 0.22$  for  $x \gg 1$ . We note that the same scaling behavior of the interface dynamics was reported in [24] for a broad family of voter models with intermediate states, as the present M-model. We have checked that the width has already reached its saturation value at the mean breaking time  $\tau_b$ , given that  $\tau_b$  is much longer than the ‘‘crossover time’’ that separates the growth and the saturation stages. Therefore, one expects that the maximum deviation of the interface should be proportional to the saturation value of the interface width, leading to the approximate scaling  $\langle d_{max} \rangle \sim L^{0.5}$ . We do not know how to explain the small discrepancy with the scaling  $\langle d_{max} \rangle \sim L^{0.525}$  obtained from simulations.

## Appendix B. Approximation of $\tau_b^{\text{III}}$ as a power law

To obtain the coefficient  $A(L_0)$  and the exponent  $\alpha(L_0)$  of the power-law approximation

$$\tau_b^{\text{III}}(L, L_0) \simeq A(L_0) L^{\alpha(L_0)} \quad (\text{B.1})$$

of  $\tau_b^{\text{III}}$  from Eq. (10) it proves useful to work on a double logarithmic scale, where

Eq. (B.1) becomes the straight line

$$y(x, x_0) \simeq \log[A(x_0)] + \alpha(x_0) x \quad (\text{B.2})$$

in the variable  $x \equiv \log(L)$ , with  $x_0 \equiv \log(L_0)$  and  $y(x, x_0) \equiv \log[\tau_b^{\text{III}}(L, L_0)]$ . Then, rewriting Eq. (10) in terms of the variables  $x$  and  $y(x)$

$$y(x) = 2 \log(1 - 2e^{-0.475x}) + 3x - \log(16d),$$

and Taylor expanding  $y(x)$  to first order in  $x - x_0$  we obtain

$$\begin{aligned} y(x) &\simeq 2 \log(1 - 2e^{-0.475x_0}) + \frac{1.9(x - x_0)}{(e^{0.475x_0} - 2)} + 3x - \log(16d) \quad (\text{B.3}) \\ &= \log\left[\frac{(1 - 2e^{-0.475x_0})^2}{16d}\right] - \frac{1.9x_0}{(e^{0.475x_0} - 2)} + \left[3 + \frac{1.9}{(e^{0.475x_0} - 2)}\right]x. \end{aligned}$$

Matching the coefficients of Eq. (B.3) with those of Eq. (B.2) and transforming back to the variable  $L_0 = e^{x_0}$  we arrive to the expressions for  $A(L_0)$  and  $\alpha(L_0)$  quoted in Eqs. (13) and (14), respectively, of the main text.

## References

- [1] R.P. Abelson. *Mathematical Models of the Distribution of Attitudes Under Controversy in Contributions to Mathematical Psychology*. New York: Rinehart Winston, 1964.
- [2] Michael Mäs and Andreas Flache. Differentiation without distancing: explaining bi-polarization of opinions without negative influence. *PLoS ONE*, 8(11):1–17, 11 2013.
- [3] P. Bonacich and P. Lu. *Introduction to Mathematical Sociology*. Princeton and Oxford: Princeton University Press, 2012.
- [4] N.P. Mark. Culture and competition: Homophily and distancing explanations for cultural niches. *Am. Sociol Rev*, 68:319–345, 2003.
- [5] A. Flache and M.W. Macy. Small worlds and cultural polarization. *J. Math Sociol*, 35:146–176, 2011.
- [6] T. Vaz Martins, M. Pineda, and R. Toral. Mass media and repulsive interactions in continuous-opinion dynamics. *EPL*, 91:48003, 2010.
- [7] Lau D. C. and Murnighan J. K. Demographic diversity and faultlines: The compositional dynamics of organizational groups. *Acad. Manag. Rev.*, 23:325, 1998.
- [8] Michael Mäs, Andreas Flache, Károly Takács, and Karen A Jehn. In the short term we divide, in the long term we unite: Demographic crisscrossing and the effects of faultlines on subgroup polarization. *Organization science*, 24(3):716–736, 2013.
- [9] M. McPherson, L. Smith-Lovin, and J. M. Cook. Birds of a feather: Homophily in social networks. *Annual Review of Sociology*, 27:415–444, 2001.
- [10] H. Ibarra. Homophily and differential returns-sex-differences in network structure and access in an advertising firm. *Administrative Science Quarterly*, 37:422–447, 1992.
- [11] Isenberg D. J. Group polarization: A critical review and meta-analysis. *Journal of personality and social psychology*, 50:1141, 1986.
- [12] A. Vinokur and E. Burnstein. Depolarization of attitudes in groups. *Journal of Personality and Social Psychology*, 36:872–885, 1978.
- [13] Myers D. G. *Group Decision Making*. Academic Press, New York, London, 1982.
- [14] C. E. La Rocca, L. A. Braunstein, and F. Vazquez. The influence of persuasion in opinion formation and polarization. *Europhys. Lett.*, 106(4):40004, 2014.
- [15] N Crokidakis and C. Anteneodo. Role of conviction in nonequilibrium models of opinion formation. *Phys. Rev. E*, 86:061127, 2012.

- [16] N. Crokidakis. Role of noise and agents' convictions on opinion spreading in a three-state voter-like model. *J. Stat. Mech.*, 2013:P07008, 2013.
- [17] P. Balenzuela, J.P. Pinasco, and V. Semeshenko. The undecided have the key: interaction-driven opinion dynamics in a three state model. *Plos One*, 10:e0139572, 2015.
- [18] G. R. Terranova, J. A. Revelli, and G. J. Sibona. Active speed role in opinion formation of interacting moving agents. *EPL*, 105:30007, 2014.
- [19] Weisbuch G, Deffuant G, Amblard F., and Nadal J.-P. Meet, discuss, and segregate! *Complexity*, 7:55, 2002.
- [20] E. Ben-Naim, P.L Krapivsky, F. Vazquez, and S. Redner. Unity and discord in opinion dynamics. *Physica A*, 330:99106, 2003.
- [21] M. Pineda, R. Toral, and E. Hernández-García. Noisy continuous-opinion dynamics. *Journal of Statistical Mechanics: Theory and Experiment*, 2009:P08001, 2009.
- [22] X. Castelló, V.M Eguíluz, and M. SanMiguel. Ordering dynamics with two non-excluding options: bilingualism in language competition. *New Journal of Physics*, 8:308, 2006.
- [23] D. Volovik and S. Redner. Dynamics of confident voting. *Journal of Statistical Mechanics: Theory and Experiment*, page P04003, 2012.
- [24] L Dall'Asta and T. Galla. Algebraic coarsening in voter models with intermediate states. *J. Phys. A: Math. Theor.*, 41:435003, 2008.
- [25] F Vazquez and C. López. Systems with two symmetric absorbing states: relating the microscopic dynamics with the macroscopic behavior. *Physical Review E*, 78:061127, 2008.
- [26] F. Vazquez, X. Castelló, and M. San Miguel. Agent based models of language competition: macroscopic descriptions and order–disorder transitions. *Journal of Statistical Mechanics: Theory and Experiment*, 2010(04):P04007, 2010.
- [27] R. Holley and T. M. Liggett. Ergodic theorems for weakly interacting infinite systems and the voter model. *Ann. Probab.*, 3:643, 1975.
- [28] I. Dornic, H. Chaté, J. Chave, and H. Hinrichsen. Critical coarsening without surface tension: The universality class of the voter model. *Phys. Rev. Lett.*, 87:045701, 2001.
- [29] J.D. Gunton, M. San Miguel, and P. S. Sahni. *Phase Transitions and Critical Phenomena*. London Academic Press, 1983.
- [30] A.J. Bray. Theory of phase-ordering kinetics. *Adv. Phys.*, 51:481, 2003.
- [31] P. Chen and S. Redner. Majority rule dynamics in finite dimensions. *Phys. Rev. E*, 71:036101, 2005.
- [32] L.F. Cugliandolo. Critical percolation in bidimensional coarsening. *Journal of Statistical Mechanics: Theory and Experiment*, 11:114001, 2016.
- [33] M. Plischke, Z. Rácz, and D. Liu. Time-reversal invariance and universality of two-dimensional growth models. *Phys. Rev. B.*, 35:3485, 1987.
- [34] V. Spirin, P.L Krapivsky, and S. Redner. Fate of zero-temperature ising ferromagnets. *Phys. Rev. E.*, 63:036118, 2001.
- [35] S. Redner. *A Guide to First-Passage Processes*. Cambridge University Press, 2001.
- [36] T.C. Schelling. Dynamic models of segregation. *J Math Sociol*, 1:143–186, 1971.
- [37] F. Family. Scaling of rough surfaces: effects of surface diffusion. *J. Phys. A: Math. Gen.*, 19:L441–446, 1986.
- [38] A.-L. Barabasi and H.E. Stanley. *Fractal Concepts in Surface Growth*. Cambridge University Press, 1995.